Superdisks in Radio Galaxies

Gopal-Krishna
National Centre for Radio Astrophysics, Tata Institute of Fundamental Research, Poona University Campus, Post Bag No. 3, Ganeshkhind, Pune 411 007, India
e-mail: krishna@ncra.tifr.res.in

and Paul J. Wiita
Department of Physics & Astronomy, Georgia State University, University Plaza, Atlanta, GA 30303-3083
e-mail: wiita@chara.gsu.edu

ABSTRACT

We present evidence for a striking new feature of powerful radio galaxies: gigantic disk-like structures of thermal gas and dust oriented roughly perpendicular to the radio jets and situated around the elliptical host galaxy. These superdisks, or fat pancakes, appear to have a typical diameter of at least 75 kpc and a width of $\sim$25 kpc. Quite plausibly, they are tidally stretched remnants of gas rich disk galaxies, or damped Lyman-α clouds, captured by the massive elliptical, and heated by its hot coronal gas.

Observational manifestations of the superdisks include the sharp, quasi-linear, edges of the radio lobes on the side facing the central elliptical, detected in at least a dozen well mapped radio galaxies at low to moderate redshifts. For radio galaxies with $z > 1.8$, evidence for superdisks is based on the apparent asymmetry of diffuse Lyα emission associated with the radio lobes, which is a very sensitive tracer of dust. This asymmetry can be understood if the brighter Lyα emission is associated with the radio lobe on the near side of the nucleus, and hence not obscured by the dust in the superdisk.

Superdisks can provide more consistent explanations for some of the best established correlations among the radio source properties, namely, the Laing-Garrington effect and the correlated radio-optical asymmetry. They are also likely to be responsible for part of the low-frequency flux variability of compact radio sources. We argue they may provide an improved explanation of Lyα absorption dips in the emission profiles of distant radio galaxies. Additional methods of searching for superdisks and testing this scenario are proposed.

Subject headings: galaxies: active — galaxies: elliptical — galaxies: interactions — galaxies: jets — ISM: dust, extinction — radio continuum: galaxies
Published in ApJ, Vol 529, pp. 189–200: 20 January 2000

1. Introduction

Counts of radio sources have demonstrated a steep rise in the co-moving number density, N_R, of classical double radio sources with redshift, z; $N_R(z \approx 1) \sim 1000 N_R(z \approx 0)$ (Jackson & Wall 1999). Recent optical imaging surveys of nearby radio galaxies (RGs) have revealed the presence of dust lanes or dusty patches in at least 50% of the RGs, suggesting that dust lanes may well turn out to be a generic feature of RGs (Goudfrooij 1994; also de Koff et al. 1996; McCarthy 1996). An intimate connection between the phenomenon of radio galaxies and the dust lanes has been suspected for the past two decades, based on the discovery of the strong tendency for the radio jets to emerge roughly perpendicular to dust lanes in at least nearby RGs (Kotanyi & Ekers 1979; Möllenhoff, Hummel & Bender 1992; Baum, Heckman & van Breugel 1992). Such considerations have led to the suggestion that the accretion of gas-rich disks by a massive elliptical galaxy provides a trigger for the ejection of non-thermal radio jets from the elliptical's nucleus (e.g., Sparks, Macchetto & Golombek 1989; Ellingson, Yee & Green 1991; Colina & de Juan 1995). One might then expect such accretion events to have been far more frequent in the past, in order to account for the strong cosmological evolution of radio sources. It is therefore important to extend the search for dust lanes in RGs to high redshifts. One practical difficulty encountered in the past was the lack of known elliptical galaxies at high redshifts, compounded by the rapid cosmological dimming of their surface brightnesses. Recent advances in finding high-z RGs have opened up the possibility of examining this question, particularly in view of the favorable circumstance that high-z RGs happen to possess powerful Lyman$-\alpha$ halos, which are very sensitive tracers of dust.

In this contribution we extend our recent attempts to discover the presence and physical properties of dusty disks in RGs over a wide range in redshift, employing high quality images taken in the Lyα and the radio continuum. We enrich the evidence for extremely large disks (with typical diameter > 75 kpc and thickness ~ 25 kpc) in over a dozen powerful RGs. (Throughout this paper we use a cosmological model with $H_0 = 75$ km s^{-1} Mpc $^{-1}$, $q_0 = 0.5$, and $\Lambda = 0$.) Being an order-of-magnitude larger than the dust lanes seen around nearby RGs such as Centaurus A and M87, these *superdisks* represent a newly identified phenomenon which may have important implications for radio source formation processes and also for some of the most striking correlations found among the radio source properties. Various pieces of this puzzle have been sketched in Gopal-Krishna et al. (1995), Gopal-Krishna & Wiita (1996) and Gopal-Krishna & Nath (1997); here we show how these and other pieces might fit together into a consistent picture and give new implications of this scenario.

Fig. 1 is a cartoon of a superdisk showing several relevant features. In §2 we discuss the disks inferred to be present in nearby RGs. Table 1 lists the evidence for superdisks, their properties and their implications for several observed phenomena, along with the sections of this paper where they are discussed. Direct detection methods are discussed in §5.5 and the main conclusions of this study are summarized in §6, where suggestions for additional work are also given.

2. Disks Found in Nearby Ellipticals

The most celebrated example of a dusty disk around a massive elliptical is the radio galaxy Cen A, where the jets emerge perpendicular to the disk. The fact that the disk is rotating much faster than the elliptical system has led to the belief that it is a product of capture of a gas-rich galaxy by the elliptical nearly a billion years ago (Junkes et al. 1993; Quinn 1991). A similar situation probably applies to other known dust-lane galaxies, where the dusty disk is kinematically and morphologically decoupled from the main body of the elliptical (e.g., Goudfrooij & DeJong 1995). Numerical models indicate that dust lanes begin to form through dissipative processes after the captured gas-rich system has completed a few orbits around the accreting galaxy, that is $\lesssim 10^9$ years after the capture begins (e.g., Steinmann-Cameron 1991; Quinn 1991; Rix & Katz 1991).

The other nearby radio galaxy, namely M87, is now also known to possess a dusty disk, as revealed by synthesis mapping in the 90 GHz continuum. This feature, also oriented normal to the radio jet, appears to be an enormously massive disk containing $\sim 10^{12} M_{\odot}$ of cold atomic gas (Despringre, Fraix-Burnet & Davoust 1996).

In spite of the difficulty of detecting absorption features such as dust lanes, unless viewed almost edge-on, they have been clearly seen in the CCD images of roughly half of the bright ellipticals observed (Sadler & Gerhard 1985; Jura et al. 1987; Ebneter, Davis & Djorgovski 1988; Goudfrooij & de Jong 1995; Zeilinger, Galletta & Madsen 1990). A similar result has been obtained from the recent *HST* survey (Baum et al. 1996; de Koff et al. 1996). While dusty disks around massive ellipticals are quite common, the maximum inferred dimension from such absorption images is obviously no bigger than the luminous main body of the elliptical (that is, a typical diameter of $\lesssim 10$ kpc; the typical measured width is ~ 1 kpc).

A trickle of information on the geometry of disks in massive ellipticals is coming from radio imaging of H I emission (Bertola et al. 1993; Pizzella et al. 1996). Again, given the limited sensitivity of such observations, the disks are seldom detected beyond the optical extent of the elliptical; however, the possibility of their extending much farther out cannot be excluded. In the following sections we present new evidence for the existence of gaseous disks associated with many ellipticals, which are an order-of-magnitude larger than the disks mentioned above.

3. Evidence for Superdisks

3.1. Radio Evidence

The ejection of anti-parallel jets from an active nucleus of an elliptical galaxy often produces a pair of radio lobes extending over tens or hundreds of kiloparsecs. Therefore, the morphologies of extended radio sources, in particular their lobes, offer a useful means to measure any structures of denser material associated with the parent galaxies. In standard models, some of the synchrotron plasma deposited by a radio jet in its terminal hot-spot flows backwards in a cocoon surrounding the jet (Scheuer 1974; Blandford & Rees 1974). Recent three-dimensional simulations (e.g., Clarke 1996; Norman 1996; Hooda & Wiita 1996, 1998) have shown that this cocoon plasma contains complex flow patterns involving vortices, and that the shocked material closest to the jet is usually dragged in the forward direction; however, much of the material somewhat farther out from the jet axis flows predominantly backward, at speeds typically $\sim$ 30% of the rate of advance of the hot-spot (e.g., Hooda & Wiita 1998; also, Scheuer 1995).

The utility of this very rarefied back-flowing synchrotron plasma as a tracer of any denser (thermal) medium associated with the host galaxy has long been recognized. In particular, it has been suggested that the lobe plasma gets deflected sideways as it impinges upon the interstellar medium of the parent elliptical galaxy (e.g., Leahy & Williams 1984; Wiita & Gopal-Krishna 1990). This is borne out by many two-dimensional hydrodynamical simulations of jets leaving galaxies, which can be carried out to much longer physical times than can be the computationally demanding 3-D models (Wiita, Rosen, & Norman 1990; Wiita & Norman 1992; Hooda, Mangalam & Wiita 1994). The occurrence of such deflections of the lobe plasma would inevitably give rise to an emission gap between the pair of lobes, in addition to sometimes producing striking morphological patterns (e.g., "wing" shapes, such as 3C 315 and 4C 12.03; Leahy & Williams 1984; Leahy & Perley 1991).

A closer scrutiny of the available high quality radio maps has led us to believe that the blocking of the back-flowing radio plasma may, in fact, frequently be caused by extremely large gaseous structures which are likely to have disk-like morphologies, quite unlike that of the ISM associated with an elliptical galaxy. This key evidence comes primarily from the detection of highly extended, sharp, and often quasi-linear, inner edges of the radio lobes on the sides facing the parent galaxy; these give rise to the appearance of strip-like emission gaps between the pair of radio lobes as long as the jet axis is close to the plane of the sky. Only a small minority of radio sources are expected to actually exhibit such sharp emission gaps between the lobe pair, because of the required orientation constraint as well as the expected fading of the lobe emission downstream from the hot-spot. Nonetheless, such sharply bounded, strip-like gaps in radio emission have been been clearly detected in several well-mapped RGs, as noted by Gopal-Krishna & Wiita (1996; hereafter GKW) and Gopal-Krishna & Nath (1997; hereafter GKN). In Table 2 we summarize some properties of an enlarged representative set of 12 such RGs. In Fig. 2 we reproduce radio images of two of them, and we urge the reader to examine published maps of the others.

The linear extents of the sharp inner edges of the radio lobes and the gaps between them provide lower limits to the diameters and widths of the postulated disks. From the radio maps of the 12 RGs which are relatively nearby ($0.03 \leq z \leq 0.69$, with $z_{median} \approx 0.15$), we infer median values of the disk diameter, $D_d \approx 75$ kpc, and disk thickness, $l_d \approx 25$ kpc. Clearly the inferred diameters are only lower limits, justifying our description of these features as *superdisks*.

Prior to their capture by the elliptical, these superdisks are likely to have been either independent disk galaxies or protogalaxies (the damped Lyman-α clouds; e.g., Wolfe et al. 1995). Their immense size after the capture is quite plausibly a result of their being tidally stretched during the process of accretion and their interaction with the hot corona of the elliptical (GKN; also §4.2), which is believed to expedite the accretion process (see, Sofue & Wakamatsu 1992).

The utility of radio maps to probe the superdisks diminishes for high-z RGs. Firstly, in that they must be highly luminous radio emitters in order to be detected in flux limited surveys, their radio structures are dominated by hot-spots, not lobes (e.g., Jenkins & McEllin 1977; Miley 1980). Secondly, due to their relatively small sizes, such distant radio sources are less well resolved, a limitation which is further exacerbated by the cosmological dimming of surface brightness, which renders the detections of the weaker inner parts of their lobes even more difficult. Fortunately, this information gap at high redshift can be bridged using optical data.

3.2. Optical Evidence

A well known tracer of dust is the Lyα emission, in that the resonant scattering greatly enhances the probability of the absorption of these photons by dust. The strong Lyα emission line is a prominent feature of most powerful RGs, and it is often found to be highly extended, spreading over several tens of kiloparsecs or more (e.g., Spinrad 1989; McCarthy 1993). Sensitive Lyα images of RGs are available for $z > 1.8$ through ground based optical observations. The extended nature of this emission provides a sensitive tracer of any dusty screen present in the foreground.

Using several examples of high-z RGs, Gopal-Krishna et al. (1995) briefly argued that the geometry of the dust distribution can be inferred from the Lyα images of those RGs in which the Lyα emission appears to be distinctly asymmetric about the active nucleus. As these provide key evidence for dusty superdisks, we now survey the most relevant details of the Lyα nebulae for an enlarged sample of high-z RGs. This sample consists of all objects of which we are aware that have published two-dimensional Lyα emission images showing substantial asymmetries; in order of increasing distance: 3C 294 ($z = 1.82$; McCarthy et al. 1990b), 3C 326.1 ($z = 1.82$; McCarthy et al. 1987); 1138−262 ($z = 2.16$; Pentericci et al. 1997); 0852+124 ($z = 2.47$; Gopal-Krishna et al. 1995); 6C 1232+39 ($z = 3.22$; Eales et al. 1993); 1243+036 ($z = 3.57$; van Ojik et al. 1996); 4C 41.17 ($z = 3.80$; Chambers, Miley, & van Breugel 1990), and 8C 1435+635 ($z = 4.26$; Lacy et al. 1994; Spinrad, Dey, & Graham 1995). The Lyα isophotes and radio maps are reproduced in Figs. 3–5 for some of these sources. The inward extensions of the radio lobes are often not visible in the high frequency radio maps shown here; however, experience with lower frequency observations shows that the lobes are often more extended towards the parent galaxy than is apparent from the high frequency maps. In this context it will be very desirable to map these distant RGs at meter wavelengths using sensitive arrays with high resolution, such as the *Giant Metrewave Radio Telescope* (GMRT) (Swarup et al. 1991).

3C 294; 1404+344 ($z = 1.82$) — This is a spectacular example of a Z-symmetric double radio source (McCarthy et al. 1990b). The Lyα emission extends over about 70 $\times$ 35 kpc^2 and is aligned with the inner radio axis. Slit-spectroscopy performed roughly along the inner radio axis clearly shows that the brighter Lyα emission, associated with the N radio lobe, is blue-shifted relative to the nucleus by up to $\sim$ 900 km s^{-1}. The weaker Lyα emission on the S side is redshifted by $\sim$ 500 km s^{-1} (McCarthy et al. 1990b). *As we shall see below, every RG with distinctly asymmetric Lyα emission (for which adequate spectroscopy has been reported) exhibits a similar kinematical pattern.*

1138–262 ($z = 2.16$) — Lyα emission covering some 75×35 kpc^2 is distinctly concentrated on the western side of the nucleus (Fig. 3; Pentericci et al. 1997). This is likely to be side of the approaching lobe, firstly because a prominent radio jet (Fig. 3) is seen on this side, and secondly, because the slit spectrum taken by Pentericci et al. shows this region of the Lyα halo to be blue-shifted by 1500–2000 km s^{-1} relative to the probable location of the radio nucleus.

OTL 0852+124 ($z = 2.47$) — The highly asymmetric Lyα halo extends over about 80 $\times$ 55 kpc^2 and is associated with the southern radio lobe (Gopal-Krishna et al. 1995). The Lyα emission shows a sharp cut-off to the N of the parent galaxy. The slit-spectroscopy along the radio axis shows that the S part of the cloud is approaching us at $\sim$ 1100 km s^{-1} relative to the parent galaxy.

4C 03.24; 1243+036 ($z = 3.57$) — Fig. 4 shows the Lyα isophotes of this RG superposed on a gray-scale radio map (van Ojik et al. 1996). The Lyα nebula extends over the entire radio source and the inner halo has dimensions of about 37 $\times$ 18 kpc^2; fainter emission is seen to extend beyond the radio source out to a distance of $\sim$ 90 kpc. Nearly all of the Lyα emission is concentrated on the southern side of the nucleus, and a slit-spectrum of this strikingly asymmetric nebulosity, taken along the radio axis, shows a negative velocity gradient of up to 2000 km s^{-1} relative to the nucleus. Again in this case, the brighter Lyα emission is on the side of the approaching lobe.

4C 41.17; 0647+415 ($z = 3.80$) — This extensively studied high-z RG is known to possess a Lyα nebula of dimensions about 45 $\times$ 30 kpc^2 (Fig 5c; Chambers et al. 1990). Here the asymmetric Lyα emission is observed predominantly from the direction of the eastern radio lobe, which should be approaching us, as it also coincides with the radio jet (Fig 5a; also see Carilli, Owen & Harris 1994). This conclusion is supported by the observed negative velocities on the eastern side, ranging up to 700 km s^{-1} relative to the nucleus, in the recently published two-dimensional velocity field measurements by Adam et al. (1997), though the sensitivity of these observations is modest. While the brighter parts of the Lyα emission could well be associated with the sheath around the jet, the asymmetry also pertains to the more extended Lyα nebulosity, which is likely to be associated with the E radio lobe (Fig. 5); good evidence for star formation triggered by the radio jet has been adduced by Dey et al. (1997). It may be noted that the presence of a dust-lane in this very distant RG has earlier been inferred from the apparent depression of Lyα and UV continuum emission (Dunlop et al. 1994; Chambers et al. 1990; Hippelein & Meisenheimer 1993);

this is also consistent with the detection of millimetric continuum emission by Chini & Krügel (1994) and Dunlop et al. (1994).

8C 1435+635 ($z = 4.26$) — This extremely distant RG is associated with a 17 kpc long radio source and faint diffuse Lyα emission showing a strong concentration to the south-east of the radio nucleus (Lacy et al. 1994; Spinrad, Dey & Graham 1995). The Lyα nebula is approximately 10 kpc long, and shows a systematic velocity gradient from the central region, with a blue-shift reaching over 1100 km s^{-1} near the S extremity of the nebula (Lacy et al. 1994).

4C 39.37; 1232+397 ($z = 3.22$) — The Lyα emission is roughly aligned with the radio axis and shows a clear asymmetry, with the preponderance of emission towards the SE radio lobe (Eales et al. 1993). Deeper radio images by Carilli et al. (1997) have failed to reveal a jet. Along with a lack of published velocity mapping, this means it is not possible at present to ascertain if the SE lobe is indeed the approaching one, as would be expected in our scheme.

3C 326.1; 1553+202 ($z = 1.825$) — This was among the first high-z RGs to be imaged in the Lyα, leading to the detection of a giant Lyα nebulosity (McCarthy et al. 1987). The nebulosity is clearly offset from the geometrical center of the radio source toward the western radio lobe. Again, neither a radio jet, nor Lyα velocity maps, have been reported for this source. From the observed Lyα asymmetry we expect that the W lobe lies on our side of the parent galaxy; therefore it is likely that a jet will eventually be found pointing towards the W lobe, and that the western region of the Lyα nebulosity will be found to be blue-shifted relative to its eastern part.

To summarize, all available examples of asymmetric Lyα halos of distant RGs have the Lyα emission appearing to arise predominantly from the near-side radio lobe. (A few other known cases of Lyα nebulae associated with distant RGs lack strong asymmetry and/or display no systematic kinematic pattern; McCarthy et al. 1996). Since there is no reason to expect a large intrinsic asymmetry in the excitation of Lyα emission, the most straightforward explanation for the observed asymmetry is that the Lyα photons arising from the farther side of the nucleus are being obscured by a large dusty disk surrounding the parent galaxy, as already inferred from the radio observations summarized above (§3.1).

4. The Lyα Nebulosity – Superdisk Connection

4.1. Origin of the Lyα nebulosities and their asymmetries

Since the spatial scales of the Lyα nebulae associated with powerful RGs are found to be correlated with the radio sizes, it seems quite plausible that the excitation of the material emitting Lyα photons is related to the radio source activity (e.g., van Ojik et al. 1996; also, Heckman et al. 1991a). Ejection of radio jets blows an expanding radio cavity though a pre-existing giant circumgalactic nebula (cf. Scheuer 1974; Carilli et al. 1994) with a two-phase density/temperature structure (Rees 1989). This creates a cocoon of filamentary nebular gas around the expanding radio lobe, which is compressed, heated, and accelerated by the lobe and its bow shock. Denser filaments within this cocoon probably manifest themselves as the Lyα nebula. Analogous scenarios have been proposed for extended [O II] and [O III] nebulosities associated with radio sources (e.g., Pedlar, Dyson & Unger 1985; Meisenheimer & Hippelein 1992). The compression wave due to the advancing shock can extend well beyond the radio hot-spots, leading to Lyα nebulosities which extend beyond the radio source. The extra large Lyα emission nebulae seen in some cases (van Ojik et al. 1997) could be associated with previous episodes of radio activity or jet instabilities cutting off the original hot-spots (e.g., Hooda, Mangalam & Wiita 1994).

The mechanisms for the excitation of the compressed circumgalactic medium include: irradiation by nuclear UV photons; shock heating by the radio jets and/or lobes; young stars whose formation was triggered by the jets; and the high energy radiation arising within the shocked medium itself (e.g., Ferland & Osterbrock 1986; Rees 1989; Begelman & Cioffi 1989; De Young 1989; Chambers & McCarthy 1990; Baum & Heckman 1989; Sutherland, Bicknell & Dopita 1993; Dey et al. 1997). We stress that the details of the ionization mechanism(s) in specific objects have no significant bearing on the interpretation presented here. The key role played by the radio lobes in both the creation and enhancement of visibility of the Lyα nebulosities (see below), is supported by the work of Heckman et al. (1991a), who found that quasars with under-developed radio lobes (i.e., $\leq$ 10 kpc) are seldom associated with spatially resolved Lyα emission.

Evidence for a sheath-like geometry of the Lyα cloud, driven from within by the expanding radio lobe, also comes from the observed splitting of the Lyα line profile in the case of the high-z RG 0852+124 (Gopal-Krishna et al. 1995). Similar arguments were made in favor of an expanding sheath of thermal plasma around the jet of the nearby RG 3C 120 (Axon et al. 1989; Akujor & Jackson 1992). In addition to the lobe-driven Lyα nebula, some of the line emission could well arise from the plasma directly compressed by the jet (e.g., 3C 120), and ionized by the nuclear UV photons. The large velocity dispersion imparted by the radio jet (or lobe) to the Lyα emitting cocoons should boost their detectability by enhancing the escape probability of the Lyα photons, which are otherwise likely to be resonantly trapped within the cocoon (Gopal-Krishna et al. 1995).

Since the formation of the Lyα nebulae appears to be linked to the radio lobes and jets, one expects to detect them on both sides of the parent galaxy of a given double radio source. The striking Lyα asymmetries observed in many sources (§3.2) could be readily understood if the Lyα emission associated with the far-side lobe is being obscured by a disk of dusty matter surrounding the parent galaxy. This interpretation is supported by the result that in all known cases of strong Lyα asymmetry where spectroscopy is available (or a radio jet is detected), the brighter emission is associated with the inferred approaching radio lobe. We must note that, as the sample of high-z RGs with detectable Lyα emission expands in the future, some counterexamples may come to light. For example, warps in the outer parts of the disk could partially occult the gas associated with the near-side radio lobe. Also, some RGs could have approaching lobes *intrinsically* much fainter in Lyα; this could happen if the radio source is small enough to be encompassed by the superdisk, or is simply too large for its lobes to be obscured along the line-of-sight.

It is worth recalling that highly extended Lyα nebulae were detected around several radio-loud quasars by Heckman et al. (1991a, b), who also found the Lyα emission to be brighter on the side of the radio jet. To explain this asymmetry, they did, in fact, invoke the possibility of dust obscuration; however, the structures of these nebulosities could not be well determined. Strong contamination from the powerful nuclear Lyα emission from the quasar component was present. Furthermore, within the standard unified scheme (e.g., Barthel 1989) the quasar jets are oriented relatively closer to the line of sight, so the Lyα emission associated with the two radio lobes would appear to be overlapping, and therefore difficult to resolve. On both of these counts, the situation is much less ambiguous in the case of RGs (cf. §3.2).

Thus, it seems quite reasonable to suppose that if the huge disks of diameter approaching 100 kpc, inferred from the examples of moderately distant radio galaxies (§3.1), were to be present also in high-z galaxies, whose radio sizes are typically no larger than 100 kpc (Kapahi 1990; Singal 1993), they could well obscure the far-side radio lobe.

4.2. Masses and expansion of the gaseous superdisks

Detection of mm and sub-mm continua provide useful estimates of dust masses in these putative giant disks, e.g., in the cases of 4C 41.17 ($z = 3.80$; Dunlop et al. 1994; Chini & Krügel 1994), and 8C 1435+635 ($z = 4.26$; Ivison et al. 1998). Similar detections have been reported for quasars (Ivison 1995; Andreani, LaFranca & Cristiani 1993), which are interpreted in terms of up to $\sim 10^{12} M_{\odot}$ of dusty material. From the evidence summarized above, this material is quite likely to be associated with the inferred superdisks.

Independent evidence for such massive gaseous disks comes from the observations of radio-loud quasars, whose far-infrared outputs are found to be a few times greater than those of radio galaxies of matched radio lobe power (Heckman, Chambers & Postman 1992). If one attributes this excess to systematically different orientations of the (optically thick) disks for RGs and QSOs, Heckman et al. estimated a gas content of $\gtrsim 10^{11} M_{\odot}$ in a kpc-scale disk component. This interpretation is not unique, and another way to understand this result would be if quasars are intrinsically stronger mid-IR emitters than RGs; this would imply the need for a more sophisticated version of the unified scheme which allows for significant non-thermal nuclear contributions to the IR emission (Heckman et al. 1992; Heckman et al. 1994). Following arguments by Eales and Edmunds (1996) and GKN (1997) and allowing for a portion of the far-IR emission to be beamed non-thermal nuclear continuum (e.g., Hes et al. 1995), we conservatively adopt $\sim 10^{10-11}\mathrm{M}_{\odot}$ as a representative value for the total gas content of the disks (and dust lanes) associated with distant RGs, but we note that a search of 14 high-z RGs provided only upper limits of $\sim 10^{11}\mathrm{M}_{\odot}$ to the gaseous content (van Ojik et al. 1997b).

The enormous diameters of the superdisks probably arise from the tidal stretching they undergo in the process of capture by the elliptical. Such huge disks, with diameters approaching 100 kpc, might be better described as “fat pancakes”, in that it is unlikely that rotational support is dominant in determining their morphologies (Rees 1997, private communication). The radio maps (e.g., Fig. 2) also suggest a median width of 20–30 kpc.

Aside from the complex merger process itself, major contributors to the huge widths include radiative and conductive heating from the hot gaseous corona of the parent elliptical and heating from the active nucleus. The high pressure of the ambient corona would compress the larger gas clumps of the captured disk to molecular cloud densities, whereas the tenuous component would be ionized and heated to 10^5–10^6K. As argued in GKN, the ensuing lateral expansion of the captured disk may well lead to a thickness of $\gtrsim 10$ kpc within 10^8–10^9 yr after its capture. Clearly, the hottest component of the disk would determine its width (see also Sparks & Collier-Cameron 1988). Evidence for thermal interaction of this kind has been reported for the nearby Sa galaxy NGC 1291, where the massive H I disk has developed a central ~ 10 kpc hole in the region occupied by the hot coronal gas (Bregman, Hogg & Roberts 1995). A source of heat input not considered by GKN is the nuclear activity itself, which would suggest that the thickest disks should be associated with RGs with the longest active lifespans.

5. Some Observational Implications of Superdisks

Although recognized only recently, superdisks can play an important role in a variety of radio source phenomena and also provide more plausible explanations of some of the best established correlations for powerful radio sources. To illustrate this we briefly recall two such possibilities discussed in GKN and GKW, and then discuss new applications.

5.1. Lobe depolarization asymmetry of radio-loud quasars

In quasars, the radio lobe on the jet side is nearly always found to depolarize less rapidly at longer radio wavelengths than does the opposite lobe (Laing 1988; Garrington et al. 1988; Garrington, Conway & Leahy 1991). The original explanation for this Laing-Garrington effect invokes a magnetoionic halo, similar to the core of the intracluster medium (ICM), around each quasar. The observed rapid depolarization of the radio lobe associated with the counter-jet is then attributed to the greater Faraday depth through which it is seen (e.g., Laing 1988; Garrington et al. 1988; Garrington & Conway 1991; also, Slysh 1966). As shown by Garrington & Conway (1991), the viability of this explanation demands that the magnetoionic halo somehow maintains a size to within a factor of two of the total extent of the expanding radio source. Furthermore, the electron density, ordered magnetic field strength, and even the existence, of a hot ICM core around all high-z radio sources is quite uncertain; the required deep X-ray observations are extremely scarce.

As an alternative to the above explanation, superdisks surrounding the RGs can be the Faraday screens. As shown by GKN, typical superdisk column densities ($\Sigma \simeq 300$ pc cm^{-3}) and magnetic fields ($B \sim 1\ \mu$G) yield an average Faraday rotation angle of $\approx 2 - 3$ rad at an emission wavelength $\lambda\ \sim\ 10$ cm where the L-G effect has been observed (see, Garrington et al. 1991). Assuming a typical scale of $d_B \sim 1$ kpc for the plasma irregularities in the superdisk (cf. Garrington & Conway 1991), GKN showed that the above parameters correspond to a Faraday dispersion parameter, $\Delta\ \approx \langle n_e^2 B^2 \rangle^{1/2} (L d_B)^{1/2} \gtrsim 10^2$ cm$^{-3}\mu$G pc, where n_e is the electron number density and L is the thickness of the disk, consistent with those inferred from the depolarization maps of quasars (cf. Table 1 of Garrington & Conway 1991). Thus, the superdisks are capable of producing the observed depolarization asymmetry in distant quasars, recalling that these disks are large enough to occult the far-side radio lobe; given that the apparent radio size of quasars at $z \gtrsim\ 1$ are ~ 60 to 70 kpc (e.g., Kapahi 1990; Singal 1993), and their radio axes are inclined, on average, at an angle of $\approx 30^\circ$ from the line-of-sight (Barthel 1989). This explanation would also obviate the need to postulate a magnetoionic corona around every high-z quasar, whose dimensions somehow remain closely matched to the steadily growing size of the radio source, as is required in the standard explanation.

5.2. The correlated radio-optical asymmetry

A number of correlations involving the arm-length ratio of RGs, $Q \equiv D_1/D_2 \geq 1$, were discussed in GKW, who showed that superdisks may provide an explanation for the striking radio-optical asymmetry correlation. As shown by McCarthy, van Breugel & Kapahi (MvBK, 1991), the peak surface brightness of the extended emission-line region (EELR) in RGs is found to occur on the side of the radio lobe which extends out to a *smaller* distance from the active nucleus. Note that the spatial extent of the EELR is typically of order of 10 kpc, comparable to the width of the superdisks described above. Moreover, the optical brightness contrast of the EELR was found to be particularly large for higher redshift sources ($z > 0.3$; McCarthy & van Breugel 1989) for which the contrast was quantified in terms of the blue emission line [O II] λ3727. This impressively tight correlation was argued by MvBK to arise from a large-scale density asymmetry of the circumgalactic medium (CGM) about the host elliptical galaxy, which would slow down the radio jet propagation more effectively on the denser side, while simultaneously enhancing the optical emissivity of the thermal filaments in the EELR on that same side (via better confinement). While this hypothesis of environmental density asymmetry is appealingly simple, GKW have argued that it is unlikely to be a complete explanation for the nearly universal (37 of 39 cases) correlation found by MvBK, on two counts. Firstly, it is difficult to understand why this correlation holds even when the lobe distance asymmetry is minute. Secondly, it is not obvious why the optical asymmetry is more pronounced for higher-z RGs whose EELRs were imaged in the (blue) [O II] λ3727 line, than it is found for the lower-z RGs imaged in the (red) Hα line.

A clue to the origin of this correlated asymmetry can be found in the data summarized in Table 2 for our sample of 12 RGs showing evidence for superdisks. Confirming the results of GKW, based on a smaller sample of RGs, we find here a strong tendency (11 out of 12) for the lobe-length asymmetry to appear systematically milder when the lobe lengths are measured from the mid-plane of the radio emission gap or superdisk mid-plane ($Q_{\rm sd}$), instead of employing the usual definition which takes the radio nucleus as the reference point (Q). In our scenario, the offset of the nucleus from the mid-plane indicates a motion of the galaxy relative to the superdisk, which is expected to result in unequal lobe lengths even in the absence of any environmental asymmetry on circum-galactic scales. The motion of the parent galaxy relative to the CGM will generate a ram pressure on the galaxy, leading to an asymmetric disposition of its (dusty) ISM. We further note here that additional sweeping of the tenuous dusty ISM could arise through the ram pressure exerted on the moving galaxy by the superdisk material. The resulting accumulation of dust on the downstream side of the moving galaxy would accentuate both the shielding of the nuclear UV photons, as well as the obscuration of the EELR radiation arising on that side, rendering its EELR emission, especially its bluer component, dimmer. At the same time, the radio lobe on that downstream side would be automatically identified as the more distant or longer one, thanks to the ongoing motion of the parent galaxy in the opposite direction. Not only would this naturally engender the observed correlated radio–optical asymmetry, but GKW showed that the strong tendency for the RGs at higher z to show a greater asymmetry of EELR emission can be readily understood, since the observed optical window would then sample shorter rest-frame wavelengths, where dust obscuration is more pronounced.

The offset of the active nucleus from the mid-plane of the superdisk would arise if the galaxy has a component of its velocity parallel to the width of the disk (GKW). Here we point out that the required velocity component should greatly exceed the sound velocity of the inertially dominant component of the superdisk. Plausibly, this latter component refers to the dust shielding molecular clouds, for which the expected sound speed is ~ 1 km s^{-1}, and the above condition is readily satisfied. If the bulk of the superdisk mass is contained in the heated gas (with $10^5{\rm K} < T < 10^6{\rm K}$; cf. §4.2), then this inequality is no longer overwhelmingly true; nonetheless, the sound velocity ($\lesssim 100$ km s^{-1}) should still be somewhat smaller than the typical galactic velocity (GKW). If the superdisk is still in the process of merging with the parent galaxy, most of its mass should be in the cold state. In this case, the motion of the accreting galaxy will be highly supersonic, and consequently the captured disk would not be greatly distorted along the direction of galaxy motion. As time goes by, the heating of the disk will gradually increase its effective sound velocity, producing some distortions in the disk shape, but by then the basic merger configuration would have been established. Quantitative estimates based on this scenario can account for the typically observed arm-length asymmetries of RGs, aside from the radio-optical correlation, without the need to postulate a universal asymmetry in the ISM/CGM of active ellipticals.

5.3. Enhanced variability by scattering

A new and potentially interesting observational effect due to the presence of superdisks involves the low-frequency intensity variations observed for flat spectrum quasars (blazars), on the time scales of several years, as reported, e.g., by Spangler et al. (1989). In particular, they found large source-to-source variations in the modulation index for sources in close proximity on the sky, even at high galactic latitudes. The inference of pronounced inhomogeneities in the turbulence properties of the Galactic ISM, is, however, not supported by pulsar observations, as noted by Spangler et al. (1989); consequently, they proposed an intrinsic origin for such slow variations. We wish to point out that the putative intrinsic variability may be the consequence of refractive scintillations arising from large-scale density inhomogeneities in the plasma of the superdisks (with $\Sigma \approx 300$ pc cm^{-3}) associated with the radio sources. Note that this electron column density is quite similar to that estimated for the line-of-sight towards Sgr A*, whose low-frequency variability has been attributed to refractive scintillations in the intervening ISM (e.g., Zhao et al. 1989). On the other hand, the expected contribution from the hot corona of the elliptical should be roughly an order-of-magnitude smaller (cf. Gopal-Krishna & Wiita 1991).

Consider now a blazar having a redshift $z = 1$ with a flux density of 1 Jy (at $\lambda = 1$ m), of which one-third arises from the compact central component. Assuming a high synchrotron opacity at meter wavelengths, the expected peak brightness temperature of $\simeq 3 \times 10^{11}$K (Readhead 1994; Singal & Gopal-Krishna 1985) would imply an angular size of $\theta \simeq 3$ mas, corresponding to a physical diameter of the central component of $d \simeq 15$ pc. As the bulk of the refractive focusing leading to the flux variability would be caused by density inhomogeneities on a characteristic scale $a \sim d$, the corresponding focusing angle, ψ, should exceed θ in order to obtain substantial flux variations, where (Scheuer 1968),

$$\psi(a) \simeq \Big(\frac{\pi^3}{2}\Big)^{1/4}\Big(\frac{L}{a}\Big)^{1/2}\alpha(a)\langle n_e\rangle r_0\lambda^2. \tag{1}$$

In this relation, $\alpha(a)\langle n_e\rangle$ is the rms fluctuation (on the scale a), of the average density $\langle n_e\rangle$, r_0 is the classical radius of the electron, and L is the depth of the refractive plasma layer. For a typical $L \simeq 20$ kpc for a superdisk, and $\langle n_e\rangle \simeq 1 \times 10^{-2}$cm^{-3}, the condition $\psi > \theta$ would require $\alpha \gtrsim 10$; this estimate is quite similar to the observationally supported value of α (~ 10) for the large scale ISM irregularities within our galaxy (Anantharamaiah & Narayan 1988). The timescale, τ, for the fluctuations would be mainly set by the apparent transverse motion of the emission knots within the compact central component. The relevant speeds are known to be often superluminal, with bulk Lorentz factor, $\Gamma \sim 10$ (Vermeulen & Cohen 1994), yielding $\tau \simeq d(1+z)/\Gamma c \sim 9$ yr. This is consistent with the estimates derived by Spangler et al. (1989) for the 'intrinsic' meter wave flux variability postulated by them. The possibility of such 'superluminal refractive scintillations' occurring in the medium outside of the galaxy has earlier been discussed in the context of plasma irregularities associated with intervening clusters of galaxies (Gopal-Krishna 1991; also, Campbell-Wilson & Hunstead 1994).

5.4. Absorption troughs in Lyα emission profiles

Another potentially important role of superdisks may be in relation to the frequent occurrence of large, often multiple, absorption dips in the Lyα emission profiles of high-z RGs with radio extent $\lesssim$ 35 kpc (9/10), but interestingly, not in larger sources (2/6), as found by van Ojik et al. (1997a). They have interpreted the absorption troughs as arising from absorption by H I clouds associated with a "molecular torus".

In our picture, these absorption features are yet another imprint of superdisks, wherein the lumps of cool gaseous material could be giving rise to the Lyα absorption (e.g., in the $z = 3.8$ RG, 4C 41.17, Dunlop et al. 1994; in the $z = 2.9$ RG, 0943−242, Röttgering et al. 1995). Indeed, the radio extents of the RGs which often show absorption dips are quite similar to the inferred widths of the superdisks and hence they are expected to provide a large covering factor for the Lyα nebulosity associated with the radio jets/lobes. Moreover, within the geometry consistent with the unified scheme (e.g., Barthel 1989), our scenario would also explain the observed rarity of the Lyα absorption troughs in the case of quasars (van Ojik et al. 1997a); the line-of-sight coverage is expected to be less effective for quasars, where the approaching lobe would be largely unobscured by the superdisk even when the overall projected radio size is comparable to the width of the disk. Another property of these absorption troughs is their observed concentration within a velocity range of $\sim$250 km s^{-1}, for a given RG (van Ojik et al. 1997a); this is similar to the typical Keplerian velocity expected within a disk, and so it too fits our scenario quite well.

5.5. Prospects for direct detection of the superdisks

Two primary sources of the heat input to the superdisks are the hot gaseous corona of the elliptical and its active nucleus. Even if most of the nuclear radiation emerges in the UV and soft X-rays it would be efficiently reprocessed into the far IR/sub-mm radiation by the dusty material of the superdisk. Similarly, the heat input from the hot corona may well generate a gaseous component of temperature 10^5–10^6 K within the superdisk (GKN), so its EUV/SX radiation would also be reprocessed by the dust into lower energy photons.

Thus the far-IR to millimeter region of the electromagnetic spectrum seems to hold the best prospects for a direct detection of the postulated superdisks. This expectation is bolstered by the successful detection of mm/sub-mm continuum from the $z = 3.8$ RG 4C 41.17 (Chini & Krügel 1994; Dunlop et al. 1994). Other detections of high-z galaxies, where thermal emission from dust appears to dominate any non-thermal continuum, have also been reported (Clements et al. 1992; Issak et al. 1994; Ivison 1995; see Eales & Edmunds 1996 for a detailed discussion).

In practice, it might be more efficient to attempt the direct detection of superdisks in relatively nearby RGs; radio sources with the morphologies discussed in §3.1 are good candidates. In these powerful sources the bolometric output of the nucleus is expected to be $\sim 10^{45}$ erg s^{-1}. Even if 1% of this is trapped by the cool dusty material of the superdisks and reradiated in the far-IR/mm region, we expect a flux density of at least a few milli-Janskys. Such levels are within the reach of the largest aperture mm-wave telescopes currently operating. Accordingly, an attempt was recently made to detect the putative superdisk in the radio galaxy 3C 33 (z = 0.0592) during the last phase of the ISO mission. Unfortunately, too little time was allocated for these 90μ observations. The resulting image appears moderately elongated by about 1 arcmin in the east-west direction (Gopal-Krishna & Altieri 1999), which is consistent with the orientation of the superdisk inferred from the radio image (Fig. 2b). *SIRTF* should provide the sensitivity needed to conduct such observations in a systematic fashion, yielding direct images. An additional approach to select candidates for superdisks is to use large millimeter telescopes to look for cold gas manifested by CO emission (e.g., Lo, Chen & Ho, 1999). Already, CO lines and dust continua have been detected from very distant objects, e.g., the QSO BR 1202−0725 ($z = 4.69$; Omont et al. 1996; Ohta et al. 1996); $\sim 10^{11}$M$_\odot$ of molecular hydrogen gas is estimated to be present.

Clearly, it will not be easy to detect the superdisk emission from the very distant sources, for which we have evidence from Lyα asymmetries. Large telescopes could provide further examples of spatially resolved Lyα velocity fields. They will also allow more measurements of line ratios that can quantify extinction due to the postulated dusty superdisks. For instance, Hα/Hβ > 20 have been measured for the EELR of the extremely luminous *IRAS* source 10214+4724 (Elston et al. 1994). Likewise, significant reddening, presumably due to dust, has been found in other high-z RGs using the Lyα/Hα ratio; values in the range 3–4 (instead of the Case B ratio of 8.75) have been measured (McCarthy, Elston & Eisenhardt 1992). Fortunately, the detection of sub-millimetric continuum due to dust is not-so-formidable a task for high-z sources, at least in comparison to measurements made at most other bands, because the dilution of the flux due to greater distance is largely offset by the steep K-correction (Braine 1995; Blain & Longair 1996). Yet another interesting pursuit would be to discover and study additional examples of very nearby lenticular galaxies with H I annuli, such as NGC 1291 (§4.2). Such data would provide observational constraints to theoretical models of the thermal interaction between the disk and coronal components surrounding the stellar bulge.

6. Conclusions and Future Directions

In this work we have taken a close look at the published high quality images of powerful radio galaxies, taken in the radio continuum and in the (resonant) Lyα line emission which is a very sensitive tracer of dust. Two striking features noticed in some of the RGs are the remarkable asymmetry of the Lyα emission across the active nucleus, and the presence of sharp, quasi-linear, edges of the radio lobes on the sides facing the parent galaxy. We argue that both of these characteristics can be consistently explained if very large, fat, disks of dusty material are present around the parent massive elliptical galaxies. From the above observations, we infer that typically these superdisks have a diameter $\gtrsim$ 75 kpc and a width of 20–30 kpc. We also show that the available kinematical evidence supports our inference that the apparent asymmetry of the Lyα emission is caused by the absorption in the superdisk of the Lyα photons arising from the nebulosity associated with the radio lobe which is located on the far side of the radio nucleus.

The limited available observational evidence indicates that these superdisks are associated with the most distant radio galaxies known, but are also present in at least some of their nearby counterparts. It may be more realistic to describe the superdisks as "fat pancakes" (which are not fully rotationally supported), quite possibly the tidally stretched remnants of captured disk galaxies or damped Lyα clouds. Conceivably, the superdisks might represent intergalactic matter accreting onto density peaks along sheet-like cosmic structures. It is an interesting question as to whether the formation of massive galaxies and the triggering of radio jets are linked to such an accretion process.

The superdisk hypothesis also helps in understanding some of the best established correlations between the properties of classical double radio sources, such as the depolarization asymmetry between the two radio lobes of quasars (the Laing-Garrington effect) and the correlated radio–optical asymmetry for FR II radio galaxies. Another important consequence of the superdisks could be the low-frequency flux variations of blazars located at high galactic latitudes. Finally, multiple absorption troughs seen in the Lyα profiles of small RGs are nicely fit by this scenario.

On the theoretical side, simulations of the accretion of massive gaseous disks onto rapidly moving elliptical galaxies would be of great interest. The heat transfer into such disks has been treated very approximately to date, and needs to be examined in greater detail. The ultimate fate of the disks over cosmological timescales is another outstanding issue. The common occurrence of these dusty disks, if confirmed, may well necessitate corrections to the reported magnitudes and colors of elliptical galaxies; for instance, *HST* images of some $z \sim 1$ RGs show extinction of rest frame UV emission at the location of the host elliptical (McCarthy 1996, and references therein).

The most interesting observational initiative would be the direct detection of some superdisks in emission. Prospects for such observations appear to be most favorable in the far-IR through millimeter bands. In particular, synthesis imaging observations of CO rich (dusty) RGs, both in CO lines and in the sub-millimeter continuum, would be very worthwhile. Also, samples of high-z RGs showing distinctly asymmetric Lyα emission should be spectroscopically mapped using very large optical telescopes, in light of our prediction that in a large majority of cases the brighter Lyα emission should be seen on the blue-shifted side of the nebula associated with the approaching radio lobe. Similarly, radio detections of jets in more such high-z RGs would enable additional tests of our hypothesis that brighter Lyα emission should be seen on the jetted side of the nucleus. It would also be very desirable to obtain more examples of RGs showing sharp emission gaps in their radio bridges; such detections will be facilitated by sensitive low-frequency synthesis telescopes such as the *GMRT*, which should best reveal the details of the older inner portions of the bridges. We have initiated some such endeavors, and urge additional search programs for the remarkable phenomena associated with superdisks.

We thank Stefi Baum, Adam Black, Ken Chambers, Robert Laing, Paddy Leahy, Laura

Pentericci, Huub Röttgering, and Hy Spinrad for giving permission to reproduce figures from their works, and, in several cases, for supplying us with postscript files. Brief discussions with Martin Rees, and Ramesh Narayan were very helpful, as were the suggestions from the referee.

G-K appreciates the hospitality of the Department of Physics & Astronomy at Georgia State University where this paper was begun, and PJW is grateful for hospitality at the National Centre for Radio Astrophysics, where the original and the revised versions were completed. This work was supported in part by NASA grant NAG 5-3098 and by Research Program Enhancement and International Strategic Initiative funds at GSU, and made use of the NASA/IPAC extragalactic database (NED) which is operated by JPL, under contract with NASA.

REFERENCES

Adam, G., Rocca-Vomerange, B., Gérard, S., Ferruit, P., & Bacon, R. 1997, A&A, 326, 501

Akujor, C. E., & Jackson, N. 1992, AJ, 104, 546

Anantharamaiah, K. R., & Narayan, R. 1988, in Radio Wave Scattering in the ISM, eds. J.M. Cordes, B.J. Rickett, D.C. Baker, (New York: AIP), 185

Andreani, P., LaFranca, F., & Cristiani, S. 1993, MNRAS, 261, L35

Axon, D. J., Pedlar, A., Unger, S. W., Meurs, E. J. A., Whittle, D. M. 1989, Nature, 341, 631

Barthel, P. D. 1989, ApJ, 336, 606

Baum, S. A., et al. 1996, in Cold Gas in the Universe, eds. M.N. Bremer, P.P. van der Werf, H.J.A. Röttgering, C.L. Carilli (Dordrecht: Kluwer), 379

Baum, S. A., & Heckman, T. 1989, ApJ, 336, 681

Baum, S. A., Heckman, T. M., & van Breugel, W. 1992, ApJ, 389, 208

Begelman, M. C., & Cioffi, D. F. 1989, ApJ, 336, 681

Bertola, F., Pizzella, A., Persic, M., & Salucci, P. 1993, ApJ, 416, L45

Black, A. R. S., Baum, S. A., Leahy, J. P., Perley, R. A., Riley, J. M., & Scheuer, P. A. G. 1992, MNRAS, 256, 186

Blandford, R. D., & Rees, M. J. 1974, MNRAS, 169, 395

Blain, A. W., & Longair M. S. 1996, MNRAS, 279, 847

Braine, J. 1995, A&A, 300, 20

Bregman, J. N., Hogg, D. E., Roberts, M. S. 1995, ApJ, 441, 561

Campbell-Wilson, D., & Hunstead, R. W. 1994, PAS Australia, 11, 33

Capetti, A., Morganti, R., Parma, P., & Fanti, R. 1993, A&A Suppl, 99, 407

Carilli, C. L., Owen, F. N. & Harris, D. E. 1994, AJ, 107, 480

Chambers, K. C., & McCarthy, P. J. 1990, ApJ, 354, L9

Chambers, K. C., Miley, G. K., & van Breugel, W. J. M. 1990, ApJ, 363, 21

Chini, R., & Krügel, E. 1994, A&A, 288, L33

Clarke, D. 1996, in Energy Transport in Radio Galaxies and Quasars, ed. P. Hardee, A. Bridle, & A. Zensus (San Francisco: ASP), 311

Clements, D. L., Rowan-Robinson, M., Lawrence, A., Broadhurst, T., & McMahon, R. 1992, MNRAS, 256, 35P

Colina, L., & de Juan, L. 1995, ApJ, 448, 548

de Koff, S. et al. 1996, ApJ Suppl, 107, 621

Despringre, V., Fraix-Burnet, D., & Davoust, E. 1996, A&A, 309, 375

Dey, A., Spinrad, H., & Dickinson, M. 1995, ApJ, 440, 515

Dey, A., van Breugel, W., Vacca, W. D., Antonucci, R. 1997, ApJ, 490, 698

De Young, D. S. 1989, ApJ, 342, L59

Dunlop, J. S., Hughes, D. H., Robbins, S., Eales, S. A., & Ward, M. J. 1994, Nature, 370, 347

Eales, S. A., & Edmunds, M. G. 1996, MNRAS, 280, 1167

Eales, S. A., Rawlings, S., Dickinson, M., Spinrad, H., Hill, G. J., & Lacy, M. 1993, ApJ, 409, 578

Ebneter, K., Davis, M., & Djorgovski, S. 1988, AJ, 95, 422

Ellingson, E., Yee, H. K. C., & Green R. F. 1991, ApJ, 371, 49

Elston, R., McCarthy, P. J., Eisenhardt, P., Dickinson, M., Spinrad, H., Januzzi, B. T., & Maloney, P. 1994, AJ, 107, 910

Ferland, G. J., & Osterbrock, D. E. 1986, ApJ, 300, 658

Garrington, S. T., & Conway, R. G. 1991, MNRAS, 250, 198

Garrington, S. T., Conway, R. G., & Leahy, J. P. 1991, MNRAS, 250, 171

Garrington, S. T., Leahy, J. P., Conway, R. G. & Laing, R. A. 1988, Nature, 331, 147

Gopal-Krishna, 1991, Current Sci., 60, 117

Gopal-Krishna, & Altieri, B. 1999, in preparation

Gopal-Krishna, Giraud, E., Melnick, J., & della Valle, M. 1995, A&A, 303, 705

Gopal-Krishna & Nath, B. B. 1997, A&A, 326, 45 (GKN)

Gopal-Krishna & Wiita, P. J. 1991, ApJ, 373, 325

Gopal-Krishna & Wiita, P. J. 1996, ApJ, 467, 191 (GKW)

Goudfrooij, P. 1994, Ph.D. dissertation, University of Amsterdam

Goudfrooij, P., & de Jong, T. 1995, A&A, 298, 784

Heckman, T. M., Chambers, K. C., & Postman, M. 1992, ApJ, 391, 39

Heckman, T. M., Lehnert, M. D., van Breugel, W., & Miley, G. K. 1991a, ApJ, 370, 78

Heckman, T. M., Lehnert, M. D., Miley, G. K., & van Breugel, W. 1991b, ApJ, 381, 373

Heckman, T. M., O'Dea, C. P., Baum, S. A., & Laurikainen, E. 1994, ApJ, 428, 65

Hes, R., Barthel, P. D. & Hoekstra, H. 1995, A&A, 303, 8

Hippelein, H., & Meisenheimer, K. 1993, Nature, 362, 224

Hooda, J. S., Mangalam, A. V., & Wiita, P. J. 1994, ApJ, 423, 116

Hooda, J. S., & Wiita, P. J. 1996, ApJ, 470, 211

Hooda, J. S., & Wiita, P. J. 1998, ApJ, 493, 81

Hughes, D. H., Dunlop, J. S., & Rawlings, S. 1997, MNRAS, 289, 766

Isaak, K. G., McMahon, R. G., Hills, R. E., Withington, S. 1994, MNRAS, 269, L28

Ivison, R. J. 1995, MNRAS, 275, L33

Ivison, R. J., et al. 1998, ApJ, 494, 211

Jackson, C., & Wall, J. V. 1999, MNRAS, 204, 160

Jenkins, C. J., & McEllin, M. 1977, MNRAS, 180, 219

Johnson, R. A., Leahy, J. P., & Garrington, S. T. 1995, MNRAS, 273, 877

Junkes, N., Haynes, R. F., Harnett, J. I., & Jauncey, D. L. 1993, A&A, 269, 29

Jura, M., Kim, D. W., Knapp, G. R., & Guhathakurta, P. 1987, ApJ, 312, L11

Kapahi, V. K. 1990, in Parsec-Scale Radio Jets, eds. J. A. Zensus and T. J. Pearson (Cambridge, Cambridge Univ. Press), 304

Kotanyi, C. G., & Ekers, R. D. 1979, A&A, 73, L1

Lacy, M. et al. 1994, MNRAS, 271, 504

Laing, R. A. 1988, Nature, 331, 149

Leahy, J. P., Black, A. R. S., Dennett-Thorpe, J., Hardcastle, M. J., Komissarov, S., Perley, R. A., Riley, J. M., & Scheuer, P. A. G. 1997, MNRAS, 291, 20

Leahy, J. P., & Perley, R. A. 1991, AJ, 102, 537

Leahy, J. P., & Williams, A. G. 1984, MNRAS, 210, 929

Lo, K.-Y., Chen, H.-W., & Ho, P. T. P. 1999, A&A, 341, 348

McCarthy, P. J. 1993, ARAA, 31, 639

McCarthy, P. J. 1996, in Cold Gas at High Redshift, eds. M.N. Bremer, P.P. van der Werf, H.J.A. Röttgering, C.L. Carilli (Dordrecht: Kluwer), p. 349

McCarthy, P. J., Baum, S. A., & Spinrad, H. 1996, ApJSupp, 106, 281

McCarthy, P. J., Elston, R., & Eisenhardt, P. 1992, ApJ, 387, L29

McCarthy, P. J., Kapahi, V. K., van Breugel, W., & Subrahmanya, C. R. 1990a, AJ, 100, 1014

McCarthy, P. J., Spinrad, H., Djorgovski, S., Strauss, M. A., van Breugel, W., & Liebert, J. 1987, ApJ, 319, L39

McCarthy, P. J., Spinrad, H., van Breugel, W., Liebert, J., Dickinson, M., & Eisenhardt, P. 1990b, ApJ, 365, 487

McCarthy, P. J., & van Breugel, W. 1989, in Extranuclear Activity in Galaxies, ed. E.J.A. Meurs & R.A.E. Fosbury (Garching bei München: ESO), 55

McCarthy, P. J., van Breugel, W., & Kapahi, V. K. 1991, ApJ, 371, 478 (MvBK)

Meisenheimer, K., & Hippelein, H. 1992, A&A, 264, 455

Miley, G. K. 1980, ARAA, 18, 165

Möllenhoff, C., Hummel, E., & Bender, R. 1992, A&A, 255, 35

Norman, M. L. 1996, in Energy Transport in Radio Galaxies and Quasars, ed. P. Hardee, A. Bridle, & A. Zensus (San Francisco: ASP), 319

Ohta, K., Yamada, T., Nakanishi, K., Kohno, K., Akiyama, M., & Kawabe, R. 1996, Nat, 382, 426

Omont, A., Pejitjean, P., Guilloteau, S., McMahon, R. G., Solomon, P. M., & Pécontal, E. 1996, Nat, 382, 428

Pedlar, A., Dyson, J. E., & Unger, S. W. 1985, MNRAS, 214, 463

Pentericci, L., Röttgering, H. J. A., Miley, G. K., Carilli, C. L., & McCarthy, P. 1997, A&A, 326, 580

Pizzella, A., Morganti, R., Sadler, E. M., & Bertola, F., 1996, in Fresh Views of Elliptical Galaxies, eds. A. Buzzoni, A. Renzini, A. Serrano (San Francisco: ASP), 53

Quinn, P. J., 1991, Nature, 349, 571

Readhead, A. C. S. 1994, ApJ, 426, 51

Rees, M. J. 1989, MNRAS, 239, 1P

Rix, H. W., & Katz, N. 1991, in Warped Disks and Inclined Rings around Galaxies, eds. S. Casertano, P.D. Sackett, F.G. Briggs (Cambridge: Cambridge Univ. Press), 112

Röttgering, H. J. A., Hunstead, R. W., Miley, G. K., van Ojik, R., & Wieringa, M. H. 1995, MNRAS, 277, 389

Sadler, E. M., & Gerhard, O. E., 1985, MNRAS, 214, 177

Scheuer, P. A. G. 1968, Nature, 218, 920

Scheuer, P. A. G. 1974, MNRAS, 166, 513

Singal, A. 1993, MNRAS, 262, L27

Singal, A., & Gopal-Krishna 1985, MNRAS, 215, 383

Slysh, V. I. 1966, Sov. Astr. 9, 533

Sofue, Y., & Wakamatsu, K.-I. 1992, PASJ, 44, L23

Spangler, S., Fanti, R., Gregorini, L., & Padrielli, L. 1989, A&A, 209, 315

Sparks, W. B., & Collier-Cameron, A. 1988, MNRAS 232, 215

Sparks, W. B., Macchetto, F., & Golombek, D. 1989, ApJ, 345, 153

Spinrad, H. 1989, in The Epoch of Galaxy Formation, ed. S. Frenk et al. (Dordrecht: Kluwer), 59

Spinrad, H., Dey, A., & Graham, J. R. 1995, ApJ, 438, L51

Steinmann-Cameron, T. Y. 1991, in Warped Disks and Inclined Rings around Galaxies, eds. S. Casertano, P.D. Sackett, F.G. Briggs, (Cambridge: Cambridge Univ. Press), 131

Sutherland, R. S., Bicknell, G. V., & Dopita, A. 1993, ApJ, 414, 510

Swarup, G., Ananthakrishnan, S., Kapahi, V. K., Rao, A. P., Subrahmanya, C. R., & Kulkarni, V. K. 1991, Current Sci., 60, 106

van Ojik, R., Röttgering, H. J. A., Carilli, C. L., Miley, G. K., & Bremer, M. N. 1996, A&A, 313, 25

van Ojik, R., Röttgering, H. J. A., Miley, G. K., & Hunstead, R. W. 1997a, A&A, 317, 358

van Ojik, R., et al. 1997b, A&A, 321, 389

Vermeulen, R. C., & Cohen, M. H. 1994, ApJ, 430, 467

Wiita, P. J., & Gopal-Krishna 1990, ApJ, 353, 476

Wiita, P. J., Rosen, A., & Norman, M. L. 1990, ApJ, 350, 545

Wolfe, A. M., Lanzetta, K. M., Foltz, C. B., & Chaffee, F. H. 1995, ApJ, 454, 698

Zeilinger, W. W., Galletta, G., & Madsen, C. 1990, MNRAS, 246, 324

Zhao, J. H., Ekers, R. D., Goss, W. M., Lo, K. Y., & Narayan, R. 1989, in The Center of the Galaxy, ed. M. Morris (Dordrecht: Kluwer), 535

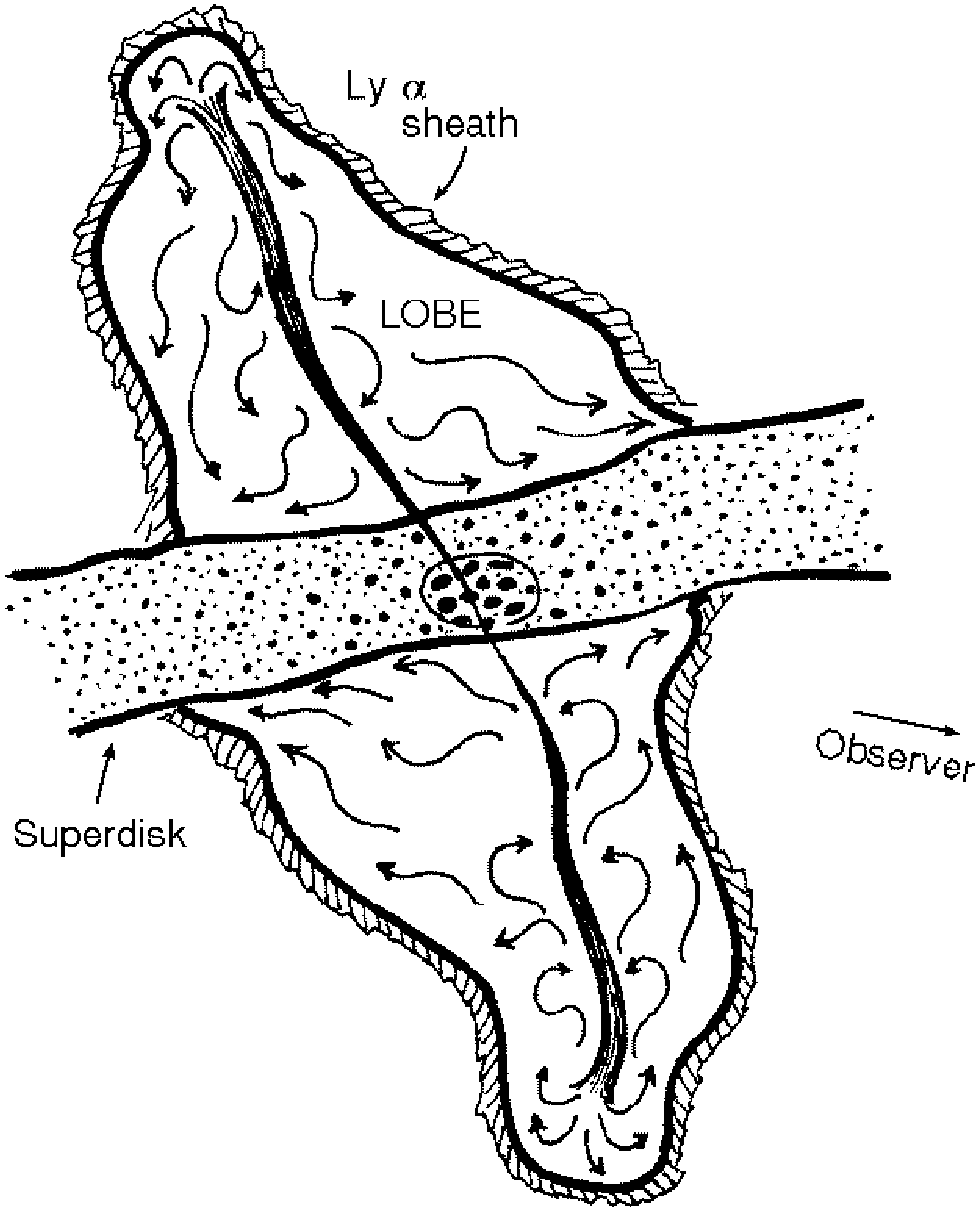

Fig. 1.— A schematic of a classical double radio source with a superdisk around the parent elliptical galaxy. The radio jets are seen emerging from the active galactic nucleus (offset from the mid-plane of the superdisk), giving rise to the two radio lobes. Note that the back-flowing synchrotron plasma is deflected sideways by the denser thermal material in the fat pancake. The shock compressed ambient plasma produces Lyα nebulosity around the radio lobes.

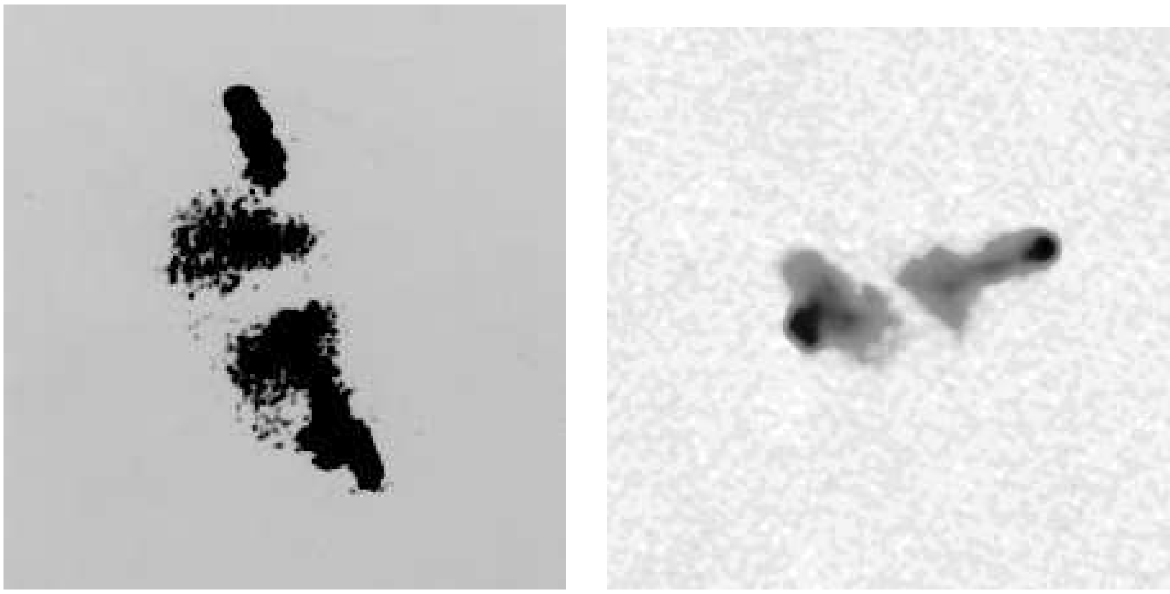

Fig. 2.— Radiophotographs of 3C 33 (left) and 4C 14.27 (right) showing clearly the sharp quasi-linear boundaries of the lobes on the sides closest to the central galaxy. Reprinted with permission from Leahy & Perley (1991), ©American Astronomical Society. The FITS files for this figure were obtained from http://www.jb.man.ac.uk/atlas maintained by Paddy Leahy, where other examples can be viewed.

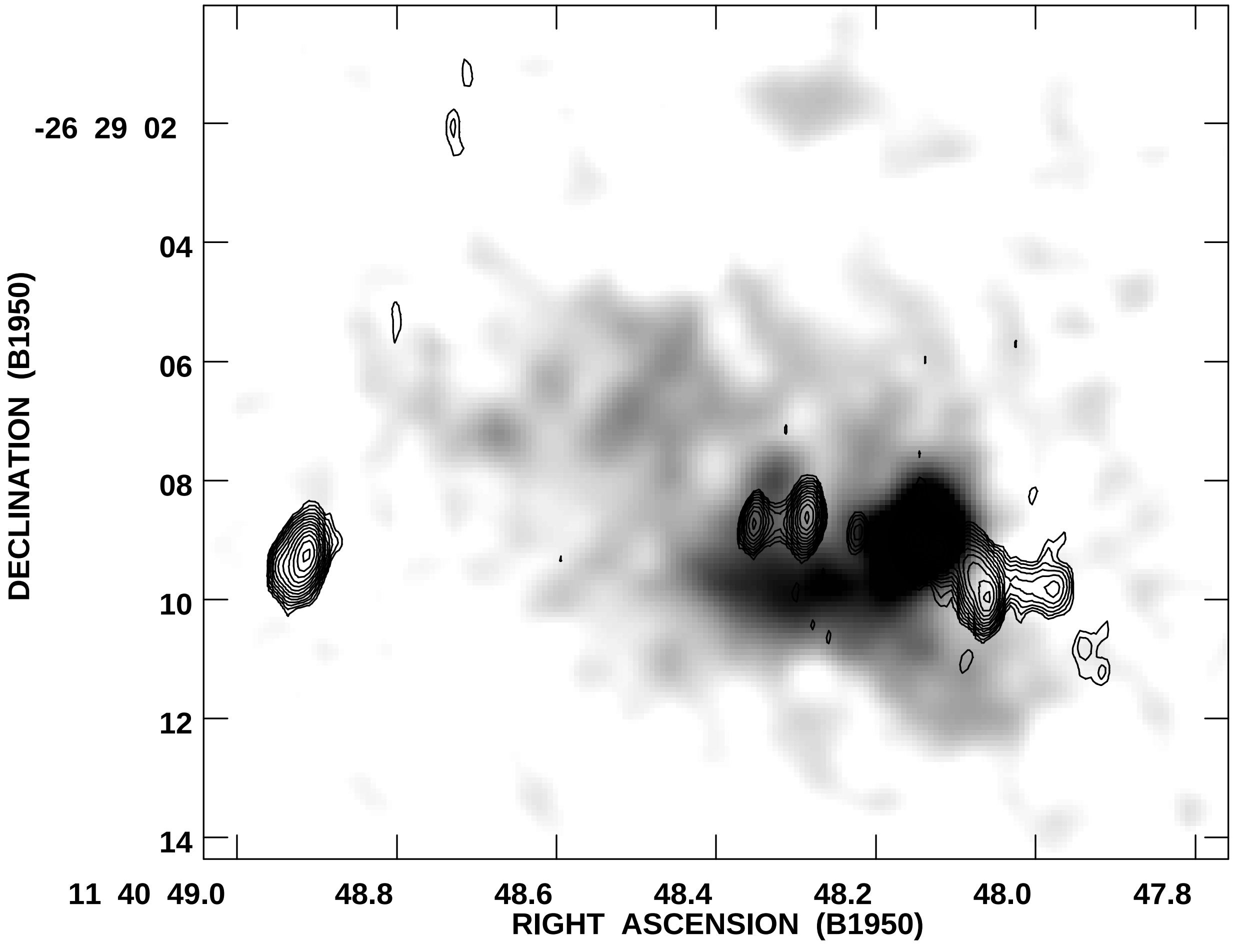

Fig. 3.— The Lyα image of 1138−262 in grayscale with the 8.1 GHz VLA map in contours superimposed. The nucleus is located at RA 11 40 48.35, DEC −26 29 08.7 (J2000), and the most intense Lyα emission hides the contours of a strong radio component (B3, in the notation of Fig. 1a of Pentericci et al. 1997). This figure was kindly provided by Laura Pentericci, and is based on two figures appearing in Pentericci et al. (1997), ©European Southern Observatory.

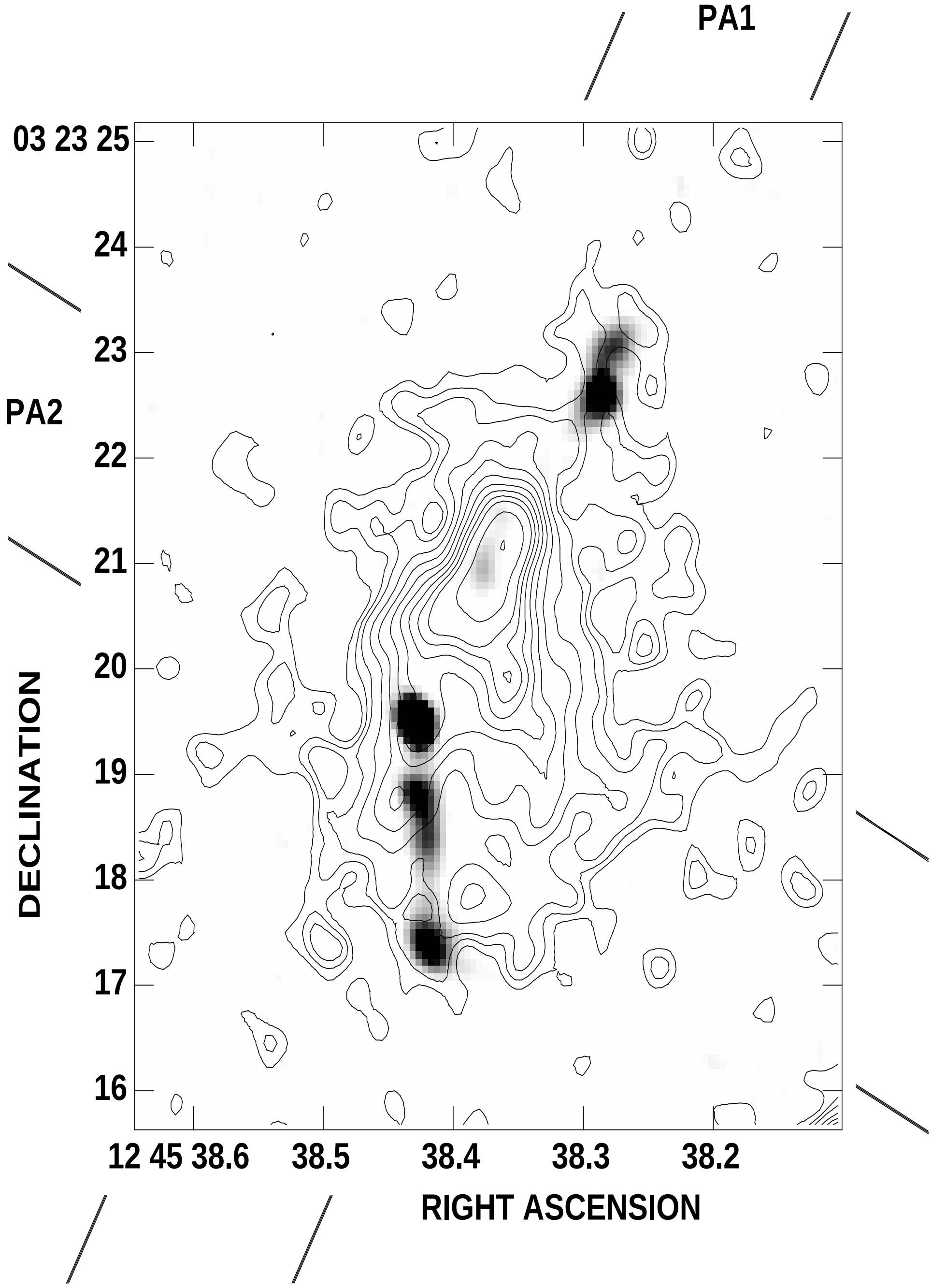

Fig. 4.— The Lyα image of 1243+036 (4C 03.24) in contours, with the 8.3 GHz VLA map in grayscale superimposed. The central peak of the Lyα contours is considered to be the nucleus. Radio component B1, the bending point of the radio structure, coincides with enhanced Lyα emission in one of the 'arms'. Indicated around the edges are the slit positions, PA1 and PA2, that were used in the high resolution spectroscopy. Reprinted with permission from van Ojik et al. (1996), ©European Southern Observatory.

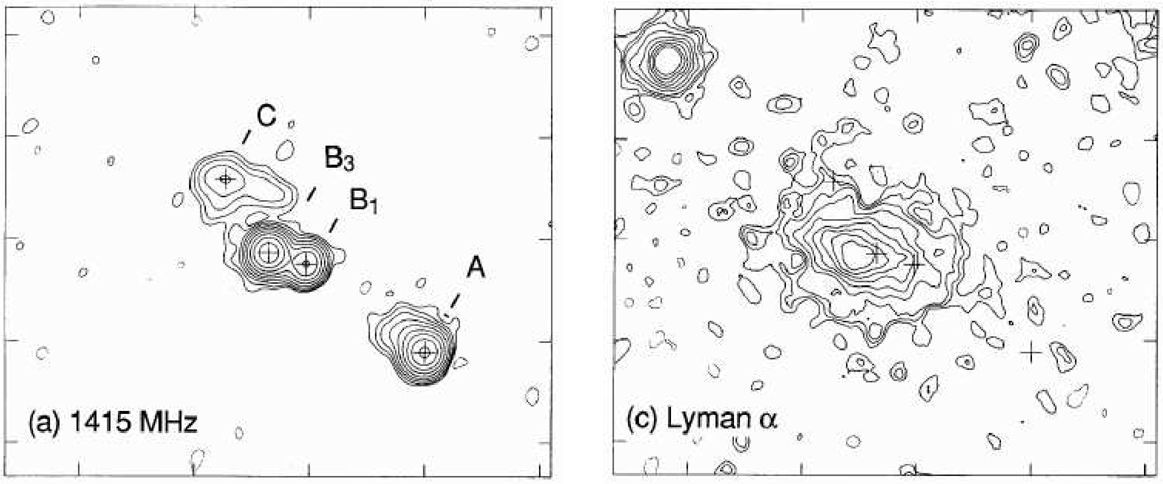

Fig. 5.— Radio (a) image of 4C 41.17 at 4.9 GHz taken with the VLA, and smoothed Lyα [labeled (c)] image on which the crosses correspond to the identified radio components. The tick marks correspond to intervals of $5''$. Reprinted with permission from Chambers et al. (1990), ©American Astronomical Society.

Table 1: The Superdisk Concept

KEY EVIDENCE	Section(s)
Sharp emission gaps seen between radio lobes of low-z RGs	3.1
Extended Lyα found stronger on near-side of high-z RGs	3.2
MAJOR PROPERTIES	
Typical widths: 20–30 kpc	3.1, 4.2
Typical diameters: $\gtrsim$ 75 kpc	3.1
Typical gaseous masses: $\gtrsim 10^{10}$ M$_\odot$	4.2
PHENOMENA EXPLAINED	
Lobe depolarization asymmetry of quasars	5.1
Correlated radio-optical asymmetry of RGs	5.2
Low frequency variability of blazars at high latitudes	5.3
Absorption troughs seen in Lyα profiles of small RGs	5.4

Table 2: Parameters of Superdisks and Radio Lobe Asymmetries

RG	z	Diameter (kpc)	Width (kpc)	Q	$Q_{\rm sd}$	References
3C 16	0.4050	56	22	2.18	1.56	1
3C 33	0.0592	45	16	1.23	1.06	1
3C 34	0.6900	70	28	1.03	1.12	2
3C 98	0.0306	30	15	1.17	1.06	3
3C 184.1	0.1182	80	45	1.33	1.16	1,3
3C 192	0.0598	80	25	1.31	1.04	3
3C 227	0.0862	85	33	1.08	1.05	4
3C 341	0.4480	53	8	1.32	1.25	1
3C 381	0.1605	45	27	1.16	1.04	1
4C 14.11	0.2070	137	30	1.20	1.06	1
4C 14.27	0.3920	80	16	1.5?	1.44	1
0828+32	0.0507	81	37	1.25	1.12	5

References. — 1) Leahy & Perley 1991; 2) Johnson et al. 1995 3) Leahy et al. 1997; 4) Black et al. 1992; 5) Capetti et al. 1993